

RUNNING TITLE: OC oxidation processes across vegetation

Carbon inputs from riparian vegetation limit oxidation of physically-bound organic carbon via biochemical and thermodynamic processes

Emily B. Graham¹, Malak M. Tfaily², Alex R. Crump¹, Amy E. Goldman¹, Evan Arntzen¹,
Elvira Romero¹, C. Tom Resch¹, David W. Kennedy¹, and James C. Stegen¹

¹Pacific Northwest National Laboratory, Richland, WA USA

²Environmental Molecular Science Laboratory, Richland, WA USA

Correspondence: Emily B. Graham, Pacific Northwest National Laboratory, PO Box 999,
Richland, WA 99352, 509-372-6049, emily.graham@pnnl.gov

Keywords: terrestrial-aquatic interface, priming, recalcitrant, labile, FT-ICR-MS, aerobic
metabolism, hyporheic zone

Key points.

- Riparian vegetation protects bound-OC stocks
- Biochemical and metabolic OC oxidation processes vary with vegetation
- Common thermodynamic principles underlie OC oxidation regardless of vegetation

1 **Abstract.**

2 In light of increasing terrestrial carbon (C) transport across aquatic boundaries, the
3 mechanisms governing organic carbon (OC) oxidation along terrestrial-aquatic interfaces are
4 crucial to future climate predictions. Here, we investigate the biochemistry, metabolic pathways,
5 and thermodynamics corresponding to OC oxidation in the Columbia River corridor using ultra-
6 high resolution C characterization. We leverage natural vegetative differences to encompass
7 variation in terrestrial C inputs. Our results suggest that decreases in terrestrial C deposition
8 associated with diminished riparian vegetation induce oxidation of physically-bound OC. We
9 also find that contrasting metabolic pathways oxidize OC in the presence and absence of
10 vegetation and—in direct conflict with the ‘priming’ concept—that inputs of water-soluble and
11 thermodynamically favorable terrestrial OC protects bound-OC from oxidation. In both
12 environments, the most thermodynamically favorable compounds appear to be preferentially
13 oxidized regardless of which OC pool microbiomes metabolize. In turn, we suggest that the
14 extent of riparian vegetation causes sediment microbiomes to locally adapt to oxidize a particular
15 pool of OC, but that common thermodynamic principles govern the oxidation of each pool (e.g.,
16 water-soluble or physically-bound). Finally, we propose a mechanistic conceptualization of OC
17 oxidation along terrestrial-aquatic interfaces that can be used to model heterogeneous patterns of
18 OC loss under changing land cover distributions.

19

20

21

22 1. Introduction

23 Soils and nearshore sediments comprise a carbon (C) reservoir that is 3.2 times larger
24 than the atmospheric C pool [*Burd et al.*, 2016], yet Earth System Models (ESMs) struggle to
25 integrate mechanisms of OC oxidation in these environments into predictions of atmospheric
26 carbon dioxide concentrations [*Todd-Brown et al.*, 2013; *Wieder et al.*, 2013; *Wieder et al.*,
27 2015]. In particular, OC oxidation in nearshore habitats constitutes a significant uncertainty in
28 atmospheric C flux [*Aalto et al.*, 2003; *Battin et al.*, 2009] and knowledge on C cycling along
29 these transitional ecosystems is necessary to accurately predict global C cycling [*Burd et al.*,
30 2016]. Terrestrial C inputs into aquatic systems have nearly doubled since pre-industrial times;
31 an estimated 2.9 Pg C now crosses terrestrial-aquatic interfaces annually (vs. 0.9 Pg C yr⁻¹ stored
32 within forested ecosystems) [*Battin et al.*, 2008; *Regnier et al.*, 2013]. The magnitude of this flux
33 has garnered significant recent attention [*Battin et al.*, 2008; *Battin et al.*, 2009; *Regnier et al.*,
34 2013], yet the biochemical, metabolic, and thermodynamic mechanisms governing OC oxidation
35 along aquatic interfaces remain a crucial uncertainty in climate predictions. New molecular
36 techniques are providing insight into OC dynamics [*Mason et al.*, 2016; *Malak M Tfaily et al.*,
37 2015; *M.M. Tfaily et al.*, 2017], but we still lack an understanding of why some OC remains
38 stabilized for millennia whereas other OC is rapidly oxidized [*Schmidt et al.*, 2011].

39 The ability of microorganisms to oxidize complex OC is an important constraint on C
40 cycling, as OC is a mixture of compounds with different propensities for biotic oxidation [*J*
41 *Hedges and Oades*, 1997; *J I Hedges et al.*, 2000]. Within terrestrial research, OC oxidation is
42 often framed within the concept of ‘priming’, whereby microbial oxidation of chemically-
43 complex, less bioavailable OC is fueled by the addition of more bioavailable and
44 thermodynamically favorable OC compounds [*Kuzyakov*, 2010]. However, the applicability of

45 priming in aquatic environments is unclear [*Bengtsson et al.*, 2014; *Bianchi*, 2011; *Guenet et al.*,
46 2010]. Aquatic systems, and in particular nearshore environments, frequently experience mixing
47 of terrestrial and aquatic C sources with distinct chemical character, providing a theoretical basis
48 for priming expectations [*Bengtsson et al.*, 2014; *Guenet et al.*, 2010]. Consistent with priming,
49 *Guenet et al.* [2010] have proposed that this mixing generates “hotspots” or “hot moments” of
50 biological activity facilitated by complementary C resources. Alternatively, OC stabilization in
51 sediments is tightly linked to organomineral interactions, which provide physical protection from
52 extracellular enzyme activity [*J I Hedges and Keil*, 1995; *Hunter et al.*, 2016; *Rothman and*
53 *Forney*, 2007], and the strength of these interactions may override any influence of priming.
54 Early investigations of priming effects in aquatic systems have been inconclusive, with evidence
55 both for [*Dorado-García et al.*, 2016] and against [*Bengtsson et al.*, 2014; *Catalán et al.*, 2015]
56 priming mechanisms.

57 Several new perspectives have attempted to move beyond frameworks, such as priming,
58 that depend on strict chemical definitions to predict OC oxidation [*Burd et al.*, 2016; *Cotrufo et*
59 *al.*, 2013; *Lehmann and Kleber*, 2015]. Recent work proposes that the probability of OC
60 oxidation is related to a spectrum of chemical properties and that even very complex OC can be
61 oxidized when more thermodynamically favorable OC is depleted or isolated from
62 microorganisms. For example, *Lehmann and Kleber* [2015] have proposed a ‘soil continuum
63 hypothesis’ whereby OC is a gradient of continually decomposing compounds that are variably
64 accessible for biotic oxidation, with no notion of chemically labile versus recalcitrant
65 compounds. Similarly, *Burd et al.* [2016] have suggested that OC oxidation is a ‘logistical
66 problem’ involving the ability of microorganisms to access and metabolize compounds. Both

67 concepts capture the emerging belief that chemically-complex, less thermodynamically favorable
68 OC can be oxidized when more favorable compounds are inaccessible.

69 Here, we address a critical knowledge gap in predicting the global C balance [*Aalto et al.*,
70 2003; *Battin et al.*, 2009; *Burd et al.*, 2016; *Regnier et al.*, 2013]—mechanisms governing OC
71 oxidation along terrestrial-aquatic interfaces. Specifically, we investigate the biochemistry,
72 microbial metabolism, and thermodynamics of OC oxidation in nearshore water-soluble and
73 physically-bound (i.e., mineral and microbial) OC pools along a freshwater terrestrial-aquatic
74 interface. We leverage natural variation in riparian vegetation along the Columbia River in
75 Eastern Washington State, the largest river in the U.S. west of the Continental Divide [*Ebel et*
76 *al.*, 1989; *Moser et al.*, 2003], to examine these mechanisms in the context of spatial variation in
77 terrestrial C deposition. Consistent with the priming paradigm, we hypothesize that (a) C
78 deposition associated with riparian vegetation increases total aerobic metabolism and enhances
79 oxidation of bound-OC stocks, while (b) areas without riparian vegetation foster lower rates of
80 aerobic metabolism with minimal oxidation of bound-OC.

81

82 **2. Materials and Methods**

83 *2.1. Site Description*

84 This study was conducted along the Columbia River shoreline within the Hanford 300
85 Area (approximately 46° 22' 15.80"N, 119° 16' 31.52"W) in eastern Washington State [*Graham*
86 *et al.*, 2016a; 2017; *Slater et al.*, 2010; *Zachara et al.*, 2013]. The Columbia River experiences
87 shoreline geographic variation in vegetation patterns, substrate geochemistry, and microbiome
88 composition [*Arntzen et al.*, 2006; *Lin et al.*, 2012; *Peterson and Connelly*, 2004; *Slater et al.*,
89 2010; *Stegen et al.*, 2016; *Stegen et al.*, 2012; *Zachara et al.*, 2013]. Accordingly, the Hanford

90 Reach of the Columbia River embodies an ideal natural system in which to examine
91 heterogeneity of terrestrial OC inputs and subsequent OC oxidation mechanisms.

92 Liquid N₂-frozen sediment profiles (0-60 cm) were collected along two shoreline
93 transects with or without riparian vegetation (hereafter, V and NV for ‘vegetated’ and ‘not
94 vegetated’, Table 1) perpendicular to the Columbia River in March 2015, separated by a distance
95 of ~170m. V was characterized by a moderately sloping scour zone, small boulders, and a closed
96 canopy of woody perennials *Morus rubra* (Red Mulberry) and *Ulmus rubra* (Slippery Elm).
97 Upper bank samples were collected within the root zone. In contrast, NV was characterized by a
98 gradually sloping scour zone, cobbled armor layer, and no vegetation. We collected profiles at
99 three locations in each transect with 5m spacing within a spatial domain of ~175 x 10m. In each
100 transect, the lower bank profile was located at ~0.5m (vertical distance) below the water line and
101 the upper bank profile was located ~0.5m (vertical distance) above the water line (approximately
102 10m horizontal distance), with the third profile situated at the midpoint. Each profile was
103 sectioned into 10-cm intervals from 0-60cm. Because OC composition (see below for Methods)
104 did not differ across upper (0-10cm) to lower (50-60cm) sections in each profile, each 10-cm
105 section was used as a replicate sample to provide sufficient sample size (n >15 at each transect)
106 for cross-site comparisons.

107

108 2.2. Sample Collection

109 Liquid N₂-frozen sediment profiles were collected as outlined in *Moser et al.* [2003]
110 using a method developed by *Lotspeich and Reed* [1980] and modified by *Rood and Church*
111 [1994]. A pointed stainless steel tube (152 cm length, 3.3 cm outside diameter, 2.4 cm inside
112 diameter) was driven into the river bed to a depth of ~60cm. Liquid N₂ was poured down the

113 tube for ~15 minutes, until a sufficient quantity of material had frozen to the outside of the rod.
114 The rod and attached material were removed from the riverbed with a chain hoist suspended
115 beneath a tripod. Profiles were placed over an aluminum foil lined cooler containing dry ice.
116 Frozen material was removed with a mallet. The material was then wrapped in the foil and
117 transported on dry ice to storage at -80°C. In the lab, profiles were sectioned into 10cm depth
118 intervals from 0-60 cm (n = 6 per profile, except for NV3 which was sectioned only from 30-
119 60cm; total n = 33)

120

121 2.3. Physicochemistry

122 Details concerning physicochemical assays are provided in the Supporting Information.
123 Briefly, we determined the particle distribution of sediments by separating size fractions via
124 sieving; total nitrogen, sulfur, and carbon content were determined using an Elementar vario EL
125 cube (Elementar Co.Germany); NH_4^+ was extracted with KCl and measured with Hach Kit
126 2604545 (Hach, Loveland, Co); iron content was measured with a ferrozine assay; and all other
127 ion concentrations were measured by inductively coupled plasma mass spectrometry (ICP-MS)
128 on HCl extractions. Aerobic metabolism was determined with a resazurin reduction assay,
129 modified from *Haggerty et al.* [2009].

130

131 2.4. FT-ICR-MS solvent extraction and data acquisition

132 We leverage state of science chemical extraction protocols combined with Electrospray
133 ionization (ESI) and Fourier transform ion cyclotron resonance (FT-ICR) mass spectrometry
134 (MS) to infer differences in OC character among our samples. Previously, *Tfaily et al.* [2015;
135 2017] have demonstrated the optimization of OC characterization from soils and sediments by

136 sequential extraction with polar and non-polar solvents tailored to the sample set of interest.
137 Tfaily's extraction procedures have been coupled to ESI FT-ICR-MS to distinguish OC pools
138 among ecosystems and soil types [Tfaily *et al.*, 2015; Tfaily *et al.*, 2017] as well as to provide
139 information on the metabolism of distinct OC pools among samples within a single environment
140 [Bailey *et al.*, 2017]. Other common OC characterization methods such as nuclear magnetic
141 resonance spectroscopy (NMR), Fourier transform infrared spectroscopy (FT-IR), and gas
142 chromatography MS only analyze a limited number of compound classes [Kögel-Knabner, 2002;
143 Kögel-Knabner, 2000]. In contrast, ESI FT-ICR-MS introduces intact organic molecules into the
144 MS without fragmentation and allows for the detection of a wide range of chemical compounds
145 [Tfaily *et al.*, 2015; Tfaily *et al.*, 2017]. The use of 12 Tesla (T) FT-ICR-MS offers high mass
146 resolving power (>1M) and mass measurement accuracy (<1 ppm), and while nascent in its
147 application within complex environmental systems, it has emerged as a robust method for
148 determining OC chemistry of natural organic matter [Kim *et al.*, 2003; Koch *et al.*, 2005; Tfaily
149 *et al.*, 2011; Tremblay *et al.*, 2007]. Moreover, Tfaily *et al.* [2015; 2017] have demonstrated that
150 sequential extraction with targeted solvents can preferentially select OC pools with differing
151 chemical character (e.g., lipid-like vs. carbohydrate-like).

152 Here, we used three solvents with different polarities —water (H₂O), methanol (CH₃OH,
153 hereafter “MeOH”) and chloroform (CHCl₃)—to sequentially extract a large diversity of organic
154 compounds from samples, according to Tfaily *et al.* [2015; 2017]. Water extractions were
155 performed first, followed by MeOH and then CHCl₃. Previous work has shown that each solvent
156 is selective towards specific types of compounds [Tfaily *et al.*, 2015]. Water is a polar solvent
157 with a selection bias for carbohydrates with high O/C ratios, amino-sugars, and other labile polar
158 compounds [Malak M Tfaily *et al.*, 2015]; and, as nearshore environments frequently experience

159 wetting, water extractions represent an estimation of readily accessible OC compounds in these
160 environments. Conversely, CHCl₃ is selective for non-polar lipids associated with mineral
161 interactions and cellular membranes (i.e., physically-bound OC) [Malak M Tfaily *et al.*, 2015].
162 Because MeOH has a polarity in between that of water and CHCl₃, it extracts both water-soluble
163 and bound-OC pools (i.e., a mix of compounds that water and CHCl₃ extract), and Tfaily *et al.*
164 [2015] have demonstrated compositional overlap between water-soluble and MeOH extracted
165 OC pools. In this study, we are interested in the differences in OC composition between pure
166 water-soluble and bound-OC pools, and we will focus our discussion on H₂O- and CHCl₃-
167 extractions only. We use H₂O- and CHCl₃-extracted OC as proxies for readily bioavailable (i.e.,
168 weakly bound) vs. less bioavailable (i.e., mineral- and microbial-bound) pools, respectively.

169 Extracts were prepared by adding 1 ml of solvent to 100 mg bulk sediment and shaking in
170 2 mL capped glass vials for two hours on an Eppendorf Thermomixer. Samples were removed
171 from the shaker and left to stand before spinning down and pulling off the supernatant to stop the
172 extraction. The residual sediment was dried with nitrogen gas to remove any remaining solvent,
173 and then the next solvent was added. The CHCl₃ and H₂O extracts were diluted in MeOH to
174 improve ESI efficiency. Tfaily *et al.* [2015] estimated the OC extraction efficiency to be ~15%.
175 Tfaily *et al.* [2015] have previously demonstrated extraction efficiencies as low as 2% to be
176 representative of OC pool composition. We further note that numerous studies have established
177 FT-ICR-MS as a robust method for distinguishing compositional differences among OC pools
178 [Herzprung *et al.*, 2017; Kellerman *et al.*, 2015; Rossel *et al.*, 2016; Ward and Cory, 2015;
179 Zhang *et al.*, 2016].

180 Ultra-high resolution mass spectrometry of the three different extracts from each sample
181 was carried out using a 12 Tesla Bruker Solarix FT-ICR-MS located at the Environmental

182 Molecular Sciences Laboratory (EMSL) in Richland, WA, USA. As per *Tfaily et al.* [2017], we
183 performed weekly calibration using a tuning solution containing $C_2F_3O_2$, $C_6HF_9N_3O$,
184 $C_{12}HF_{21}N_3O$, $C_{20}H_{18}F_{27}N_3O_8P_3$, and $C_{26}H_{18}F_{39}N_3O_8P_3$ with m/z ranging from 112 to 1333
185 (Agilent Technologies, Santa Clara, CA USA), and instrument settings were optimized using
186 Suwannee River Fulvic Acid (IHSS). The instrument was flushed between samples using a
187 mixture of water and methanol. Blanks were analyzed at the beginning and the end of the day to
188 monitor for background contaminants.

189 The extracts were injected directly into the mass spectrometer and the ion accumulation
190 time was optimized for all samples to account for differences in OC concentration. The ion
191 accumulation time ranged between 0.5 and 1s. A standard Bruker electrospray ionization (ESI)
192 source was used to generate negatively charged molecular ions. Samples were introduced to the
193 ESI source equipped with a fused silica tube (30 μm i.d.) through an Agilent 1200 series pump
194 (Agilent Technologies) at a flow rate of 3.0 $\mu L \text{ min}^{-1}$. Experimental conditions were as follows:
195 needle voltage, +4.4 kV; Q1 set to 50 m/z ; and the heated resistively coated glass capillary
196 operated at 180 °C.

197

198 2.5. FT-ICR-MS data processing

199 One hundred forty-four individual scans were averaged for each sample and internally
200 calibrated using an organic matter homologous series separated by 14 Da ($-CH_2$ groups). The
201 mass measurement accuracy was less than 1 ppm for singly charged ions across a broad m/z
202 range (100-1200 m/z). The mass resolution was $\sim 350K$ at 339 m/z . Data Analysis software
203 (BrukerDaltonik version 4.2) was used to convert raw spectra to a list of m/z values applying

204 FTMS peak picker module with a signal-to-noise ratio (S/N) threshold set to 7 and absolute
205 intensity threshold to the default value of 100.

206 Putative chemical formulae were then assigned using in-house software following the
207 Compound Identification Algorithm (CIA), proposed by *Kujawinski and Behn* [2006], modified
208 by *Minor et al.* [2012], and previously described in *Tfaily et al.* [2017]. Chemical formulae were
209 assigned based on the following criteria: $S/N > 7$, and mass measurement error < 1 ppm, taking
210 into consideration the presence of C, H, O, N, S and P and excluding other elements. To ensure
211 consistent formula assignment, we aligned all sample peak lists for the entire dataset to each
212 other in order to facilitate consistent peak assignments and eliminate possible mass shifts that
213 would impact formula assignment. We implemented the following rules to further ensure
214 consistent formula assignment: (1) we consistently picked the formula with the lowest error and
215 with the lowest number of heteroatoms and (2) the assignment of one phosphorus atom requires
216 the presence of at least four oxygen atoms.

217

218 2.6. Identification of putative biochemical transformations using FT-ICR-MS

219 To identify potential biochemical transformations, we followed the procedure detailed by
220 *Breitling et al.* [2006] and employed by *Bailey et al.* [2017]. In essence, the mass difference
221 between m/z peaks extracted from each spectrum with $S/N > 7$ were compared to commonly
222 observed mass differences associated with biochemical transformations. All possible pairwise
223 mass differences were calculated within each extraction type for each sample, and differences
224 (within 1ppm) were matched to a list of 92 common biochemical transformations (e.g., gain or
225 loss of amino groups or sugars, Table S1). For example, a mass difference of 99.07 corresponds
226 to a gain or loss of the amino acid valine, while a difference of 179.06 corresponds to the gain or

227 loss of a glucose molecule. Pairs of peaks with a mass difference within 1 ppm of our
228 transformation list were considered to be related by the corresponding compound. This approach
229 is feasible with FT-ICR-MS data because the set of peaks in each sample are related by
230 measureable and clearly defined mass differences corresponding to gains and losses of
231 compounds. It has been previously used by *Bailey et al.* [2017] to demonstrate differences in
232 biochemical transformations among soils incubated with different microbial inoculate and among
233 pore size classes in complex soil matrices.

234

235 *2.7. Identification of putative microbial metabolic pathways using FT-IR-MS*

236 Additionally, a set of putative microbial metabolic pathways in each sample can be
237 identified by locating chemical formulae assigned to m/z 's within metabolic pathways defined in
238 the Kyoto Encyclopedia of Genes and Genomes (KEGG, Release, 80.0, <http://www.kegg.jp>)
239 [*Kanehisa and Goto*, 2000]. Chemical formulae were mapped to KEGG pathways using an in-
240 house software to detect all KEGG pathways containing a giving formula. For example, a peak
241 with a mass of 400.3356 was assigned formula $C_{20}H_{16}O_9$ and mapped to KEGG pathway
242 'map00254' (Aflatoxin biosynthesis) which contains $C_{20}H_{16}O_9$ as an intermediate. While only a
243 subset of compounds detected by FT-ICR-MS are defined within the KEGG database (i.e., peaks
244 must be assigned a chemical formula and that chemical formula must be present in a KEGG
245 pathway), we found 415 unique peaks that were assigned putative molecular formulae *and* that
246 corresponded to compounds present in KEGG pathways. Additionally, we defined assignments
247 at the pathway level (i.e., by "map" number) instead of using enzyme level classification (i.e.,
248 EC number) in order to aggregate compounds found within the same pathways. This was done to
249 facilitate functional interpretation.

250 Although we acknowledge our results do not represent a comprehensive analysis of all
251 microbial metabolic pathways present in a sample, we assume that KEGG pathways containing
252 more peaks detected by FT-ICR-MS within a sample are more likely to be active than those with
253 fewer mapped peaks. We further reduced possible random matches by assessing correlations
254 with aerobic metabolisms as described in the ‘Statistical Methods’ section below, and we
255 compare results across samples to yield insight into microbial pathways in each sample beyond
256 that which can be garnered from biochemical transformations. The results are, however,
257 conceptually congruent with those derived from the biochemical transformation analyses
258 described in the preceding sub-section. The KEGG pathway and transformation analyses are
259 independent of each other, yet provided consistent insights and thus together they provide greater
260 confidence in our interpretations.

261

262 *2.8. Statistical Methods*

263 All statistical analyses were conducted using R software (<https://www.r-project.org/>). FT-
264 ICR m/z intensities were converted into presence/absence data prior to analysis because
265 differences in m/z intensity are influenced by ionization efficiency as well as relative abundance
266 [Kujawinski and Behn, 2006; Minor et al., 2012; Malak M Tfaily et al., 2015; M.M. Tfaily et al.,
267 2017].

268 To examine differences in OC composition between transects, we used the ‘vegan’
269 package to construct a Sorenson dissimilarity matrix for all m/z’s identified (i.e., we included
270 peaks with or without assigned formula) within each OC pool (water-soluble or physically-
271 bound). Differences between vegetation states (i.e., V vs. NV) were tested with PERMANOVA
272 (999 permutations, ‘vegan’) and visualized using Non-metric Multidimensional Scaling (NMDS,

273 ‘vegan’). One sample (NV, profile 1, depth 30-40cm) was removed due to peak interference
274 during FT-ICR-MS, and three samples (NV, profile 2, depths 00-10cm, 10-20cm, 20-30cm) were
275 excluded, because we were unable to collect sufficient sample mass for all analyses.

276 To reveal transformations associated with aerobic metabolism and to study differences in
277 those transformations across vegetation states, we determined the number of times a given
278 transformation occurred within each OC pool in each sample. Specifically, for each of the 92
279 compounds in our set of biochemical transformations, we counted the number of times in each
280 sample that transformation was observed to yield an estimate of the prevalence or ‘abundance’ of
281 each transformation in each sample. We correlated these abundance estimates to rates of
282 metabolism using Pearson’s product-moment correlation coefficient. Positive relationships were
283 inferred as biochemical transformations possibly associated with biotic OC oxidation. To
284 evaluate how transformations associated with OC oxidation varied across vegetation states we
285 used the abundances of those transformations across all samples to calculate Bray-Curtis
286 dissimilarity. Resulting Bray-Curtis dissimilarities were used to visual multivariate differences
287 among samples using non-metric Multidimensional Scaling (NMDS, ‘vegan’), and we
288 statistically evaluated separation between vegetation states with PERMANOVA (999
289 permutations, ‘vegan’). We refer to H₂O- and CHCl₃-soluble OC pools at V and NV,
290 respectively, as V-W (‘vegetated water’), V-B (‘vegetated bound’), NV-W (‘not vegetated
291 water’), and NV-B (‘not vegetated bound’) for the remainder of the manuscript.

292 Similar to our analyses of biochemical transformations, we found the number of m/z’s
293 that mapped to a given KEGG pathway. We make the assumption that pathways with more m/z’s
294 mapped to them have a higher probability of actively contributing to biogeochemical function.
295 To identify which pathways were most likely to contribute to aerobic metabolism, we correlated

296 the number of m/z's mapped to a given KEGG pathway within each sample to aerobic
297 metabolism. Those pathways with positive correlations were interpreted as contributing to OC
298 oxidation, and the following analysis was conducted only with KEGG pathways that positively
299 correlated with aerobic metabolism. The number of peaks mapping to each KEGG pathway in a
300 sample was normalized by the total number of peaks mapping to any positively correlated KEGG
301 pathway in the sample to yield data as a relative abundance. To reveal groups of pathways co-
302 varying with each other across vegetation states and OC pools, we statistically clustered
303 pathways that positively correlated with aerobic metabolism. Clustering was based on pathway
304 relative abundances in each vegetation state and pool type. Clusters were determined using the
305 'hclust' algorithm in R with the 'complete linkage' clustering method and visualized using the
306 'pheatmap' package.

307 Finally, we examined associations between aerobic metabolism and OC thermodynamics
308 by calculating the Gibbs Free Energy of OC oxidation under standard conditions ($\Delta G^{\circ}_{\text{COX}}$) from
309 the Nominal Oxidation State of Carbon (NOSC) as per *La Rowe and Van Cappellen* [2011].
310 NOSC was calculated from the number of electrons transferred in OC oxidation half reactions
311 and is defined by the equation:

$$312 \quad (1) \text{NOSC} = -((-Z + 4a + b - 3c - 2d + 5e - 2f)/a) + 4$$

313 , where a, b, c, d, e, and f are, respectively, the numbers of C, H, N, O, P, S atoms in a given
314 organic molecule and Z is net charge of the organic molecule (assumed to be 1). In turn, $\Delta G^{\circ}_{\text{COX}}$
315 was estimated from NOSC following *La Rowe and Van Cappellen* [2011]:

$$316 \quad (2) \Delta G^{\circ}_{\text{COX}} = 60.3 - 28.5(\text{NOSC})$$

317 Values of $\Delta G^{\circ}_{\text{COX}}$ are generally positive, indicating that OC oxidation must be coupled to the
318 reduction of a terminal electron acceptor. While $\Delta G^{\circ}_{\text{COX}}$ varies according to the availability of

319 terminal electron acceptors, our system is primarily oxic, allowing us to infer oxygen as the
320 primary electron acceptor in most reactions and make direct comparisons across samples.
321 Additionally, though the exact calculation of $\Delta G^{\circ}_{\text{CoX}}$ necessitates an accurate quantification of all
322 species involved in every chemical reaction in a sample, the use of NOSC as a practical basis for
323 determining $\Delta G^{\circ}_{\text{CoX}}$ has been validated [Arndt *et al.*, 2013; LaRowe and Van Cappellen, 2011].

324 Here, we assessed relationships between aerobic metabolism and $\Delta G^{\circ}_{\text{CoX}}$ of OC
325 compounds identified in each OC pool (determined by FT-ICR-MS analysis) using linear
326 regressions in each vegetation state, in which aerobic metabolism was the independent variable
327 and average $\Delta G^{\circ}_{\text{CoX}}$ of all m/z's with assigned formula was the dependent variable.

328

329 **3. Results and Discussion**

330 *3.1. Shifts in physicochemical, metabolic, and OC character between vegetation states*

331 Differences in vegetation states corresponded to differences in physicochemistry, aerobic
332 metabolism, and OC pool composition. V was characterized by mature trees near the water line
333 and was nutrient-rich relative to NV (Figure S1-3). V displayed comparatively high
334 concentrations of total C and rates of aerobic metabolism (Figure S1-3). In contrast, NV
335 consisted of vegetation-free, cobble-ridden shoreline with sandier soils, low total C, and low
336 aerobic metabolism (Figure S1-3).

337 Compositional difference in OC pools indicated a possibility for distinct OC oxidation
338 processes between the vegetation states (Figure 1), as preferential oxidation of certain OC
339 compounds in each state would be expected to generate an observable difference in OC pool
340 composition. Further, total organic OC content explained only 38% of aerobic metabolic rates
341 ($R^2 = 0.38$, $P < 0.0001$, Figure S4), leaving open the possibility that OC compositional

342 differences may be related to differences in aerobic metabolism at each vegetation state. The
343 following sections explore this possibility.

344

345 *3.2. Associations between C transformations and aerobic metabolism*

346 Given compositional differences in OC between vegetation states and known impacts of
347 C chemistry on metabolic functioning in other systems [*Castle et al.*, 2016; *Graham et al.*,
348 2016b], we hypothesized that biochemical transformations related to rates of aerobic metabolism
349 would be unique to each vegetation state.

350 Consistent with this hypothesis, transformation analysis indicated that the biochemical
351 processes associated with OC oxidation were significantly different between the vegetation
352 states. Specifically, OC transformations that increased in abundance with increases in aerobic
353 metabolism were significantly different at each vegetation state (PERMANOVA, H₂O P = 0.022
354 and CHCl₃ P = 0.002, Figure 3 a-b, Table 2). In comparing differences in transformations
355 occurring within the water-soluble OC pool, we observed higher abundances of amino- and
356 sugar-associated transformations for V-W relative to NV-W. Twenty-six of these
357 transformations were identified as contributing to aerobic metabolism in V-W, while none were
358 identified in NV-W. These V-W transformations were primarily associated with simple C
359 molecules (e.g., glucose, alanine, and lysine, Table 2). Conversely, within the bound-OC pool,
360 38 transformations were identified as contributing to aerobic metabolism in NV-B, compared to
361 only 11 in V-B. In both cases, these transformations consisted of a greater proportion of complex
362 C molecules (e.g., pyridoxal phosphate, palmitic acid, and glyoxylate, Table 2) than in water-
363 soluble pools.

364 The larger number of transformations associated with aerobic metabolism in V-W vs. V-
365 B, and the larger number in NV-B vs. NV-W, suggests that aerobic metabolism in vegetated and
366 unvegetated areas depend on water-soluble and bound-OC pools, respectively. We note some
367 oxidation of the bound-OC pool under vegetated conditions, but only 11 correlations were
368 observed between V-B transformations and aerobic metabolism suggesting a relatively minor
369 role, especially considering that there were 38 significant correlations for NV-B.

370 These differences suggest that an increased supply of bioavailable compounds in
371 vegetated areas leads to bound-OC being less involved in aerobic metabolism, relative to
372 unvegetated areas where bound-OC appears to be heavily involved in aerobic metabolism. The
373 concept of priming [Kuzuyakov, 2010] would predict the opposite pattern—a greater supply of
374 bioavailable OC should increase the contributions of less bioavailable OC (here, bound-OC) to
375 aerobic metabolism. Our results run counter to a priming mechanism and indicate that the supply
376 of bioavailable compounds—potentially derived from riparian vegetation—diminishes the
377 contribution of bound-OC to aerobic metabolism and, in turn, protects bound-OC pools. Mineral-
378 stabilized OC therefore has greater potential to remain sequestered along river corridors with
379 spatially and temporally consistent inputs of bioavailable OC, potentially derived from riparian
380 vegetation. The fate of OC that moves across the terrestrial-aquatic continuum may therefore be
381 impacted by land use change [Foley *et al.*, 2005] in ways not currently represented in ESMs.

382

383 *3.3. Associations between microbial metabolic pathways and aerobic metabolism*

384 Because we observed stark differences in the identity of OC transformations that
385 correlated with aerobic metabolism across vegetation states, we hypothesized that the microbial
386 metabolic pathways associated with OC transformations were also dependent on vegetation state.

387 Indeed, pathways associated with OC oxidation were distinct at V vs. NV, supporting our
388 hypothesis that there were differences in the metabolic processing of OC in the presence or
389 absence of riparian vegetation. Specifically, while the metabolism of plant-derived compounds
390 appeared to be a major driver of aerobic respiration at both vegetation states, metabolism at V
391 mostly involved readily bioavailable plant derivatives in the water-soluble OC pool, and
392 metabolism at NV was associated with plant derivatives in the bound-OC pool (Figure 4).

393 In V-W, two primary pathways were involved in metabolism of plant compounds, each
394 contained within its own hierarchical cluster (map01110: Biosynthesis of secondary metabolites;
395 map00941: Flavonoid biosynthesis). An additional cluster of plant-associated metabolisms with
396 lower abundance in V-W (Cluster 4) was also positively correlated to aerobic metabolism
397 (Figure 4). Each of these pathways denotes an association between plant-derived compounds and
398 OC oxidation in sediments. Secondary metabolites (map01110) are largely comprised of plant-
399 derived compounds such as flavonoids [Agati *et al.*, 2012], terpenoids [Tholl, 2015], and
400 nitrogen-containing alkaloids [Willaman and Schubert, 1961], while flavonoids [Agati *et al.*,
401 2012] are one of those most abundant plant-derived compounds. Associations with aflatoxin
402 [Trail *et al.*, 1995], flavone/flavonol [Agati *et al.*, 2012], and phenylpropanoids [Hahlbrock and
403 Scheel, 1989] (Cluster 4) bolster this association between plant-associated metabolic pathways
404 and aerobic metabolism in V-W.

405 Although correlations between plant-associated KEGG pathways and aerobic metabolism
406 could indicate the persistence of plant secondary metabolites rather than microbial metabolism,
407 our results indicate a central role for vegetation in water-soluble OC oxidation in either case. For
408 example, if KEGG associations were attributable to plant metabolism instead of microbial
409 metabolism, correlations between plant-associated pathways and aerobic metabolism in V-W

410 would indicate an indirect relationship between plant growth and microbial oxidation of OC,
411 whereby plant byproducts support microbial communities in oxidizing other portions of the OC
412 pool.

413 In contrast to V-W, NV-W did not display associations between plant-associated
414 metabolic pathways and OC oxidation. All significant correlations in NV-W indicated broad
415 metabolic processes including membrane transport and carbohydrate metabolism that may
416 indicate utilization of other resources (Cluster 3, Figure 4).

417 Instead, we observed relationships between plant-associated metabolisms and OC
418 oxidation within NV-B. For example, correlations with aerobic metabolism were strongest in
419 Cluster 1, which contained pathways of cutin, suberine, and wax biosynthesis [*King et al.*, 2007;
420 *Raffaele et al.*, 2009; *Shepherd and Wynne Griffiths*, 2006], alpha-linolenic acid metabolism
421 [*Crawford et al.*, 2000; *Creelman and Mulpuri*, 2002], and biosynthesis of secondary metabolites
422 [*Agati et al.*, 2012; *Tholl*, 2015; *Willaman and Schubert*, 1961] (Figure 4). Each of these
423 pathways denotes the synthesis or metabolism of a plant-associated lipid compound. Because no
424 specific metabolisms were correlated to OC oxidation in NV-W, we hypothesize that these lipid-
425 based metabolisms comprise the primary KEGG-identifiable pathways associated with OC
426 oxidation in areas without riparian vegetation. We also observed one cluster of pathways that
427 correlated with metabolism at V-B (Cluster 7) and contained plant-associated metabolic
428 pathways such as linoleic acid metabolism [*Crawford et al.*, 2000; *Creelman and Mulpuri*, 2002]
429 and brassinosteroid biosynthesis [*Bishop*, 2007], indicating some oxidation of lipid plant material
430 in the bound-OC pool under vegetated conditions. We therefore propose that plant-derived lipid
431 compounds serve as a secondary substrate for OC oxidation in shorelines with riparian
432 vegetation, given that most correlations at V were detected in the water-soluble pool.

433

434 *3.4. Thermodynamics of carbon oxidation*

435 Finally, we hypothesized that microbes would preferentially oxidize more
436 thermodynamically favorable compounds at both sites, consistent with common thermodynamic
437 constraints on biogeochemical cycles [Burgin *et al.*, 2011; Hedin *et al.*, 1998; Helton *et al.*,
438 2015]. Because we observed evidence for preferential OC oxidation of the water-soluble OC
439 pool at V and of the bound-OC pool at NV, we further hypothesized that thermodynamic-based
440 preference of OC oxidation would be observable only in the preferred substrate pool within each
441 vegetation state. Consistent with this hypothesis, aerobic metabolism was positively correlated to
442 average $\Delta G^{\circ}_{\text{Cox}}$ in V-W ($R^2 = 0.22$, $P = 0.03$, Fig 5a) and NV-B ($R^2 = 0.54$, $P = 0.001$ Fig 5b),
443 but these variables were not correlated in V-B or NV-W. In both cases, aerobic metabolism
444 corresponded to a depletion of more thermodynamically favorable OC (i.e., OC became less
445 favorable as aerobic metabolism increased), resulting in progressively less favorable
446 thermodynamic conditions.

447 The priming conceptual framework would predict that terrestrial inputs associated with
448 riparian vegetation should condition microbial communities to oxidize less thermodynamically
449 favorable C, such as that found in the bound-OC pool. In such a scenario, inputs of
450 thermodynamically favorable carbon should—by minimizing community-level energy
451 constraints—allow for the rise of microbial physiologies that can oxidize less favorable C
452 [Kuznyakov, 2010]. In this case, a significant relationship between thermodynamic favorability
453 and aerobic metabolism in the V-W pool should lead to a similar relationship within the V-B
454 pool. Our results reveal a strong relationship within the V-W pool, but not in the V-B pool,

455 thereby rejecting an influence of priming. Instead, our results suggest that bound-OC pools are
456 protected by thermodynamically favorable compounds that serve as preferred substrate.

457 In contrast to our expectation that water-soluble OC associated with riparian vegetation
458 would increase oxidation of bound-OC pools, we observed evidence consistent with inhibition of
459 bound-OC oxidation by thermodynamically favorable water-soluble compounds. Priming has
460 been actively debated in aquatic research [*Bengtsson et al.*, 2014; *Bianchi*, 2011; *Guenet et al.*,
461 2010], and a number of other studies have been unable to detect a priming effect in sediment and
462 aqueous habitats [*Bengtsson et al.*, 2014; *Catalán et al.*, 2015].

463 The mechanisms resulting in priming are not well understood, but the phenomenon has
464 been associated with nutrient and energy limitations in soil environments [*Kuzyakov*, 2010]. For
465 instance, under nutrient limitation microorganisms may oxidize chemically-complex OC to
466 garner resources (e.g., nitrogen mining), while shared resources that facilitate OC oxidation (e.g.,
467 extracellular enzymes) are more likely to facilitate ecological cheating under energy limiting
468 conditions [*Blagodatskaya and Kuzyakov*, 2008; *Catalán et al.*, 2015; *Guenet et al.*, 2010;
469 *Kuzyakov*, 2010]. Our system is oligotrophic, containing a fraction of the total C content
470 observed in other systems (Figure S1) such that C limitation rather than nutrient limitation might
471 drive OC oxidation dynamics. In such a case, readily bioavailable C inputs would be rapidly
472 oxidized but microbial communities may be well-adapted to rely on alternative energy sources
473 (e.g., NH_4^+ , Fe) that may be more available than bound-OC pools.

474

475 3.5. Conceptual model for OC oxidation at terrestrial-aquatic interfaces

476 Based on our work, we propose a conceptual model of OC oxidation along terrestrial-
477 aquatic interfaces in which the oxidation of bound-OC is limited by terrestrial inputs from

478 riparian vegetation (Fig 6. a-b). Riparian vegetation sustains inputs of water-soluble compounds
479 to nearshore OC pools, resulting in a larger thermodynamically favorable, water-soluble OC pool
480 (Figure 6b). This leads to higher overall C content in nearshore sediments and elevated rates of
481 aerobic respiration relative to areas with less riparian vegetation. However, our data suggest that
482 in the presence of riparian vegetation microbial carbon oxidation primarily uses the water-
483 soluble OC pool with minimal oxidation of bound-OC due to physical and/or thermodynamic
484 protection of this pool. For instance, $\Delta G^{\circ}_{\text{Cox}}$ was lower in water-soluble OC pools than in bound-
485 OC, and a large presence of this thermodynamically favorable pool may provide adequate
486 substrate to sustain metabolic functioning, limiting the need to metabolize less
487 thermodynamically favorable OC. Additionally, organomineral interactions can protect bound-
488 OC from extracellular enzyme activity [Hunter *et al.*, 2016], inhibiting the bioavailability of
489 OC.

490 In contrast, non-vegetated riparian zones provide little input into water-soluble OC pools
491 (Fig 6a), and rates of metabolism and C pool sizes are lower in these environments. Carbon
492 oxidation in these non-vegetated zones occurs primarily within the bound-OC pool, albeit more
493 slowly and as product of different biochemical and metabolic pathways than in vegetated
494 environments (e.g., complex C transformations and lipid-based metabolism of plant derivatives).
495 We posit that water-soluble pools in non-vegetated sediments are sufficiently small that investing
496 in enzymes needed to metabolize this OC pool results in a net energy loss. Instead, microbes in
497 unvegetated areas must investment in cellular machinery to access bound-OC, and our results
498 imply that the cellular machinery needed to access bound-OC is distinct from the machinery
499 needed to access water-soluble OC.

500 Interestingly, aerobic metabolism within both types of sediments is related to a depletion
501 of thermodynamically favorable compounds; however, this occurs in water-soluble OC pools in
502 vegetated zones and bound-OC pools in non-vegetated zones. That is, microorganisms in both
503 environments are constrained to the metabolism of their primary substrate pool but preferentially
504 oxidize more thermodynamically favorable compounds within that pool. This suggests that
505 microorganisms are conditioned to metabolize a subset of compounds within sediment OC,
506 possibly defined by thermodynamic or physical protection mechanisms, but operate under
507 common thermodynamic constraints once adapted to oxidize a certain OC pool.

508

509 *3.6. Broader Implications*

510 Our results indicate that terrestrial C inputs associated with riparian vegetation protect
511 bound-OC from oxidation, possibly aiding long-term storage of mineral-bound pools along river
512 corridors, and our work is particularly relevant to global patterns of CO₂ emissions in light of
513 changes in land cover and increases in C fluxes across the terrestrial-aquatic interface. The
514 magnitude, distribution, and chemical quality of terrestrial C fluxes into aquatic environments
515 are perturbed by shifts in land cover (e.g., due to agriculture, urbanization, and climate-driven
516 vegetation change) [Fang *et al.*, 2005; Knapp *et al.*, 2008]. These fluxes have been examined
517 primarily for their own propensity to be oxidized along land-to-sea continuums [Battin *et al.*,
518 2008; Battin *et al.*, 2009; Regnier *et al.*, 2013], but we also suggest a role for these fluxes in
519 stabilizing mineral-bound carbon within nearshore environments. For example, vegetation
520 removal, impervious surfaces, and drainage systems coincident with urbanization alter terrestrial
521 C runoff patterns, both changing their magnitude and creating preferential deposition flow paths
522 [Fraleay *et al.*, 2009; Imberger *et al.*, 2011; Smith and Kaushal, 2015]. Agricultural drainage

523 systems also lead to preferential flow paths as well as spatiotemporal variation in the quantity
524 and quality of terrestrial-aquatic fluxes [*Graeber et al.*, 2012; *Larson et al.*, 2014], an effect that
525 strongly influences C cycling given that 40% of the earth's land is cultivated [*Foley et al.*, 2005;
526 *Graeber et al.*, 2012]. We propose that changes in the distribution of these fluxes through space
527 and time may impact OC oxidation both in the C transported along these flow paths and within
528 sediments that are differentially exposed to terrestrial OC.

529 Furthermore, vegetation distributions in natural ecosystems are predicted to shift in
530 response to altered precipitation regimes. Associated changes in plant phenology, morphology,
531 and establishment will impact the quantity, quality, and distribution of terrestrial material
532 entering aquatic systems [*Knapp et al.*, 2008], and we currently have an incomplete
533 understanding of how these patterns will vary across ecosystems and precipitation patterns [*Fang*
534 *et al.*, 2005; *Knapp et al.*, 2008]. A mechanistic framework for C oxidation that captures impacts
535 of heterogeneity in vegetation in river corridors will therefore aid in predicting how terrestrial-
536 aquatic interfaces respond to ongoing perturbations. Here, we demonstrate a potential for
537 increases in the intensity of terrestrial C fluxes to lead to larger mineral-bound C pools by
538 physically and thermodynamically protecting these pools; and conversely, a potential for
539 oxidation of mineral-bound C pools in areas with diminished terrestrial C inputs.

540 Earth System Models depend on mathematical representations of C cycling, and the
541 continued development of these models is tightly coupled to conceptual advances drawn from
542 field-based observations [*Burd et al.*, 2016; *Six et al.*, 2002]. Despite recent progress, these
543 models are still missing key regulatory processes [*Todd-Brown et al.*, 2013; *Wieder et al.*, 2013;
544 *Wieder et al.*, 2015]. To address this knowledge gap, we propose a new conceptual framework of
545 OC dynamics based on analysis of *in situ* observational data that explicitly considers a central

546 challenge in model improvement—biochemical, metabolic, and thermodynamic mechanisms
547 governing OC oxidation along terrestrial-aquatic interfaces. Our results directly contrast those
548 expected within a ‘priming’ framework, and we advance that water-soluble thermodynamically
549 favorable OC associated with riparian vegetation protects thermodynamically less favorable
550 bound-OC from oxidation. We also demonstrate differences in biochemical and metabolic
551 pathways associated with metabolism of water-soluble and bound-OC pools in the presence or
552 absence of riparian vegetation, furthering a processed-based understanding of terrestrial-aquatic
553 interfaces.

554 Our conceptualization of OC oxidation may also be applicable beyond terrestrial-aquatic
555 interfaces, as many ecosystems experience spatiotemporal variability in the quantity of
556 thermodynamically favorable water-soluble OC. For instance, vegetation senescence generates
557 pulses of bioavailable C into most temperate and tropical ecosystems. Our research provides an
558 opportunity to enhance the mechanistic underpinning of OC oxidation process representations
559 within ESMs—an imperative under heterogeneous landscapes and unknown future land cover
560 distributions—and proposes interactions between OC thermodynamics and mineral-inhibition of
561 OC oxidation as a key future research need.

562

563 **Author Contributions.**

564 EBG was responsible for conceptual development and data analysis and was the primary writer
565 with guidance from JCS and MT. ARC, AEG, CTR, ECR, DWK, and JCS were responsible for
566 experimental design and data collection. MT was responsible for all FT-ICR processing. All
567 authors contributed to manuscript revisions.

568

569 **Acknowledgements.**

570 This research was supported by the US Department of Energy (DOE), Office of
571 Biological and Environmental Research (BER), as part of Subsurface Biogeochemical
572 Research Program's Scientific Focus Area (SFA) at the Pacific Northwest National
573 Laboratory (PNNL). PNNL is operated for DOE by Battelle under contract
574 DE-AC06-76RLO 1830. A portion of the research was performed at Environmental Molecular
575 Science Laboratory User Facility. We thank Nancy Hess for helpful feedback in manuscript
576 revision.
577

578 **References.**

579

580 Aalto, R., L. Maurice-Bourgoin, T. Dunne, D. R. Montgomery, C. A. Nittrouer, and J.-L. Guyot
581 (2003), Episodic sediment accumulation on Amazonian flood plains influenced by El
582 Nino/Southern Oscillation, *Nature*, 425(6957), 493-497.

583 Agati, G., E. Azzarello, S. Pollastri, and M. Tattini (2012), Flavonoids as antioxidants in plants:
584 location and functional significance, *Plant Science*, 196, 67-76.

585 Arndt, S., B. B. Jørgensen, D. E. LaRowe, J. Middelburg, R. Pancost, and P. Regnier (2013),
586 Quantifying the degradation of organic matter in marine sediments: a review and synthesis,
587 *Earth-science reviews*, 123, 53-86.

588 Arntzen, E. V., D. R. Geist, and P. E. Dresel (2006), Effects of fluctuating river flow on
589 groundwater/surface water mixing in the hyporheic zone of a regulated, large cobble bed river,
590 *River Research and Applications*, 22(8), 937-946.

591 Bailey, V. L., A. Smith, M. Tfaily, S. J. Fansler, and B. Bond-Lamberty (2017), Differences in
592 soluble organic carbon chemistry in pore waters sampled from different pore size domains, *Soil*
593 *Biology and Biochemistry*, 107, 133-143.

594 Battin, T. J., L. A. Kaplan, S. Findlay, C. S. Hopkins, E. Marti, A. I. Packman, J. D. Newbold,
595 and F. Sabater (2008), Biophysical controls on organic carbon fluxes in fluvial networks, *Nature*
596 *Geoscience*, 1(2), 95-100.

597 Battin, T. J., S. Luyssaert, L. A. Kaplan, A. K. Aufdenkampe, A. Richter, and L. J. Tranvik
598 (2009), The boundless carbon cycle, *Nature Geoscience*, 2(9), 598-600.

599 Bengtsson, M. M., K. Wagner, N. R. Burns, E. R. Herberg, W. Wanek, L. A. Kaplan, and T. J.
600 Battin (2014), No evidence of aquatic priming effects in hyporheic zone microcosms, *Scientific*
601 *reports*, 4, 5187.

602 Bianchi, T. S. (2011), The role of terrestrially derived organic carbon in the coastal ocean: A
603 changing paradigm and the priming effect, *Proceedings of the National Academy of Sciences*,
604 108(49), 19473-19481.

605 Bishop, G. J. (2007), Refining the plant steroid hormone biosynthesis pathway, *Trends in plant*
606 *science*, 12(9), 377-380.

607 Blagodatskaya, E., and Y. Kuzyakov (2008), Mechanisms of real and apparent priming effects
608 and their dependence on soil microbial biomass and community structure: critical review,
609 *Biology and Fertility of Soils*, 45(2), 115-131.

610 Breitling, R., S. Ritchie, D. Goodenowe, M. L. Stewart, and M. P. Barrett (2006), Ab initio
611 prediction of metabolic networks using Fourier transform mass spectrometry data,
612 *Metabolomics*, 2(3), 155-164.

613 Burd, A. B., S. Frey, A. Cabre, T. Ito, N. M. Levine, C. Lønborg, M. Long, M. Mauritz, R. Q.
614 Thomas, and B. M. Stephens (2016), Terrestrial and marine perspectives on modeling organic
615 matter degradation pathways, *Global change biology*, 22(1), 121-136.

616 Burgin, A. J., W. H. Yang, S. K. Hamilton, and W. L. Silver (2011), Beyond carbon and
617 nitrogen: how the microbial energy economy couples elemental cycles in diverse ecosystems,
618 *Frontiers in Ecology and the Environment*, 9(1), 44-52.

619 Castle, S. C., D. R. Nemergut, A. S. Grandy, J. W. Leff, E. B. Graham, E. Hood, S. K. Schmidt,
620 K. Wickings, and C. C. Cleveland (2016), Biogeochemical drivers of microbial community
621 convergence across actively retreating glaciers, *Soil Biology and Biochemistry*, 101, 74-84.

- 622 Catalán, N., A. M. Kellerman, H. Peter, F. Carmona, and L. J. Tranvik (2015), Absence of a
623 priming effect on dissolved organic carbon degradation in lake water, *Limnology and*
624 *Oceanography*, 60(1), 159-168.
- 625 Cotrufo, M. F., M. D. Wallenstein, C. M. Boot, K. Deneff, and E. Paul (2013), The Microbial
626 Efficiency - Matrix Stabilization (MEMS) framework integrates plant litter decomposition with
627 soil organic matter stabilization: do labile plant inputs form stable soil organic matter?, *Global*
628 *Change Biology*, 19(4), 988-995.
- 629 Crawford, M., C. Galli, F. Visioli, S. Renaud, A. P. Simopoulos, and A. A. Spector (2000), Role
630 of plant-derived omega-3 fatty acids in human nutrition, *Annals of Nutrition and Metabolism*,
631 44(5-6), 263-265.
- 632 Creelman, R. A., and R. Mulpuri (2002), The oxylipin pathway in Arabidopsis, *The Arabidopsis*
633 *Book*, e0012.
- 634 Dorado-García, I., J. Syväranta, S. P. Devlin, J. M. Medina-Sánchez, and R. I. Jones (2016),
635 Experimental assessment of a possible microbial priming effect in a humic boreal lake, *Aquatic*
636 *Sciences*, 78(1), 191-202.
- 637 Ebel, W. J., C. D. Becker, J. W. Mullan, and H. L. Raymond (1989), The Columbia River--
638 toward a holistic understanding, *Canadian special publication of fisheries and aquatic*
639 *sciences/Publication speciale canadienne des sciences halieutiques et aquatiques*. 1989.
- 640 Fang, J., S. Piao, L. Zhou, J. He, F. Wei, R. B. Myneni, C. J. Tucker, and K. Tan (2005),
641 Precipitation patterns alter growth of temperate vegetation, *Geophysical research letters*, 32(21).
- 642 Foley, J. A., R. DeFries, G. P. Asner, C. Barford, G. Bonan, S. R. Carpenter, F. S. Chapin, M. T.
643 Coe, G. C. Daily, and H. K. Gibbs (2005), Global consequences of land use, *science*, 309(5734),
644 570-574.
- 645 Fraley, L. M., A. J. Miller, and C. Welty (2009), Contribution of In - Channel Processes to
646 Sediment Yield of an Urbanizing Watershed1, *JAWRA Journal of the American Water Resources*
647 *Association*, 45(3), 748-766.
- 648 Graeber, D., J. Gelbrecht, M. T. Pusch, C. Anlanger, and D. von Schiller (2012), Agriculture has
649 changed the amount and composition of dissolved organic matter in Central European headwater
650 streams, *Science of the Total Environment*, 438, 435-446.
- 651 Graham, E. B., A. R. Crump, C. T. Resch, S. Fansler, E. Arntzen, D. W. Kennedy, J. K.
652 Fredrickson, and J. C. Stegen (2016a), Coupling spatiotemporal community assembly processes
653 to changes in microbial metabolism, *Frontiers in Microbiology*, 7, 1949.
- 654 Graham, E. B., A. R. Crump, C. T. Resch, S. Fansler, E. Arntzen, D. W. Kennedy, J. K.
655 Fredrickson, and J. C. Stegen (2017), Deterministic influences exceed dispersal effects on
656 hydrologically - connected microbiomes, *Environmental Microbiology*, 19(4), 1552-1567.
- 657 Graham, E. B., J. E. Knelman, R. S. Gabor, S. Schooler, D. M. McKnight, and D. Nemergut
658 (2016b), Dissolved organic matter and inorganic mercury loadings favor novel methylators and
659 fermentation metabolisms in oligotrophic sediments, *bioRxiv*, 072017.
- 660 Guenet, B., M. Danger, L. Abbadie, and G. Lacroix (2010), Priming effect: bridging the gap
661 between terrestrial and aquatic ecology, *Ecology*, 91(10), 2850-2861.
- 662 Haggerty, R., E. Martí, A. Argerich, D. Von Schiller, and N. B. Grimm (2009), Resazurin as a
663 "smart" tracer for quantifying metabolically active transient storage in stream ecosystems,
664 *Journal of Geophysical Research: Biogeosciences*, 114(G3).
- 665 Hahlbrock, K., and D. Scheel (1989), Physiology and molecular biology of phenylpropanoid
666 metabolism, *Annual review of plant biology*, 40(1), 347-369.

- 667 Hedges, J., and J. Oades (1997), Comparative organic geochemistries of soils and marine
668 sediments, *Organic geochemistry*, 27(7), 319-361.
- 669 Hedges, J. I., G. Eglinton, P. G. Hatcher, D. L. Kirchman, C. Arnosti, S. Derenne, R. P.
670 Evershed, I. Kögel-Knabner, J. De Leeuw, and R. Littke (2000), The molecularly-
671 uncharacterized component of nonliving organic matter in natural environments, *Organic*
672 *Geochemistry*, 31(10), 945-958.
- 673 Hedges, J. I., and R. G. Keil (1995), Sedimentary organic matter preservation: an assessment and
674 speculative synthesis, *Marine chemistry*, 49(2-3), 81-115.
- 675 Hedin, L. O., J. C. von Fischer, N. E. Ostrom, B. P. Kennedy, M. G. Brown, and G. P. Robertson
676 (1998), Thermodynamic constraints on nitrogen transformations and other
677 biogeochemical processes at soil-stream interfaces, *Ecology*, 79(2), 684-703.
- 678 Helton, A. M., M. Ardón, and E. S. Bernhardt (2015), Thermodynamic constraints on the utility
679 of ecological stoichiometry for explaining global biogeochemical patterns, *Ecology letters*,
680 18(10), 1049-1056.
- 681 Herzsprung, P., K. Osterloh, W. von Tümpling, M. Harir, N. Hertkorn, P. Schmitt-Kopplin, R.
682 Meissner, S. Bernsdorf, and K. Friese (2017), Differences in DOM of rewetted and natural
683 peatlands—Results from high-field FT-ICR-MS and bulk optical parameters, *Science of The Total*
684 *Environment*, 586, 770-781.
- 685 Hunter, W. R., R. Niederdorfer, A. Gernand, B. Veuger, J. Prommer, M. Mooshammer, W.
686 Wanek, and T. J. Battin (2016), Metabolism of mineral - sorbed organic matter and microbial
687 lifestyles in fluvial ecosystems, *Geophysical Research Letters*.
- 688 Imberger, S. J., R. M. Thompson, and M. R. Grace (2011), Urban catchment hydrology
689 overwhelms reach scale effects of riparian vegetation on organic matter dynamics, *Freshwater*
690 *Biology*, 56(7), 1370-1389.
- 691 Kanehisa, M., and S. Goto (2000), KEGG: kyoto encyclopedia of genes and genomes, *Nucleic*
692 *acids research*, 28(1), 27-30.
- 693 Kellerman, A. M., D. N. Kothawala, T. Dittmar, and L. J. Tranvik (2015), Persistence of
694 dissolved organic matter in lakes related to its molecular characteristics, *Nature Geoscience*,
695 8(6), 454-457.
- 696 Kim, S., R. W. Kramer, and P. G. Hatcher (2003), Graphical method for analysis of ultrahigh-
697 resolution broadband mass spectra of natural organic matter, the van Krevelen diagram,
698 *Analytical Chemistry*, 75(20), 5336-5344.
- 699 King, A., J.-W. Nam, J. Han, J. Hilliard, and J. G. Jaworski (2007), Cuticular wax biosynthesis
700 in petunia petals: cloning and characterization of an alcohol-acyltransferase that synthesizes
701 wax-esters, *Planta*, 226(2), 381-394.
- 702 Knapp, A. K., C. Beier, D. D. Briske, A. T. Classen, Y. Luo, M. Reichstein, M. D. Smith, S. D.
703 Smith, J. E. Bell, and P. A. Fay (2008), Consequences of more extreme precipitation regimes for
704 terrestrial ecosystems, *Bioscience*, 58(9), 811-821.
- 705 Koch, B. P., M. Witt, R. Engbrodt, T. Dittmar, and G. Kattner (2005), Molecular formulae of
706 marine and terrigenous dissolved organic matter detected by electrospray ionization Fourier
707 transform ion cyclotron resonance mass spectrometry, *Geochimica et Cosmochimica Acta*,
708 69(13), 3299-3308.
- 709 Kögel-Knabner, I. (2002), The macromolecular organic composition of plant and microbial
710 residues as inputs to soil organic matter, *Soil Biology and Biochemistry*, 34(2), 139-162.
- 711 Kögel-Knabner, I. (2000), Analytical approaches for characterizing soil organic matter, *Organic*
712 *Geochemistry*, 31(7), 609-625.

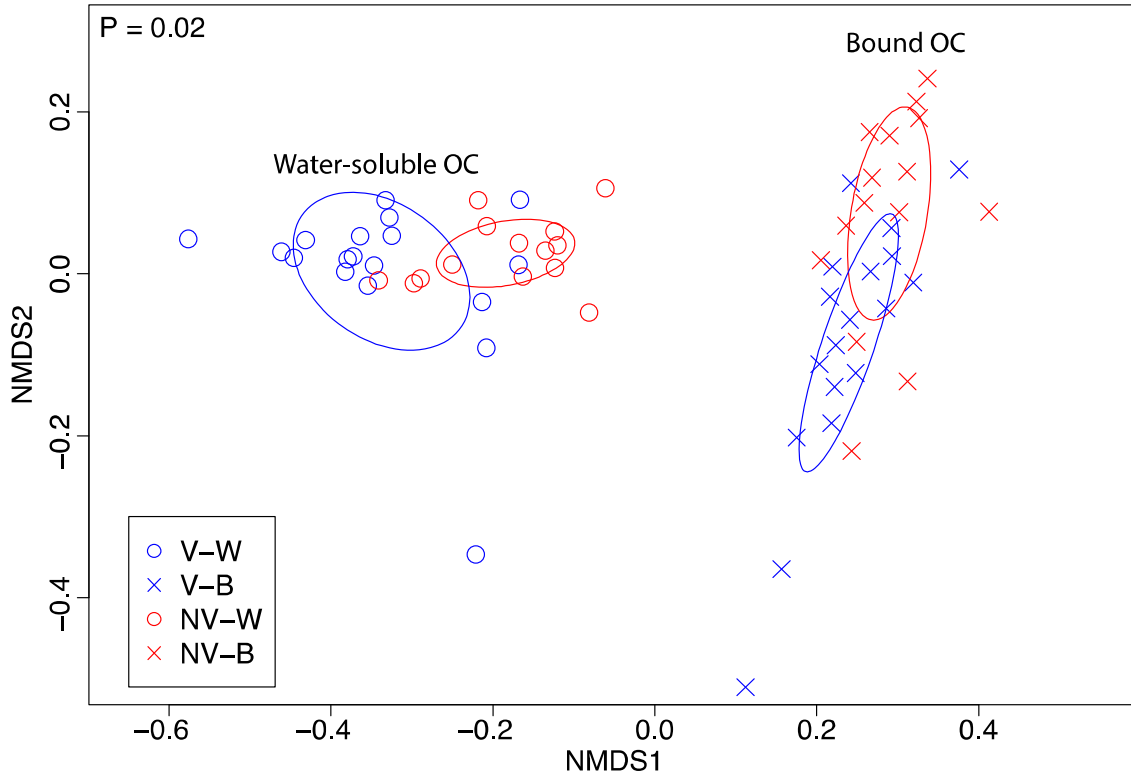
- 713 Kujawinski, E. B., and M. D. Behn (2006), Automated analysis of electrospray ionization
714 Fourier transform ion cyclotron resonance mass spectra of natural organic matter, *Analytical*
715 *Chemistry*, 78(13), 4363-4373.
- 716 Kuzyakov, Y. (2010), Priming effects: interactions between living and dead organic matter, *Soil*
717 *Biology and Biochemistry*, 42(9), 1363-1371.
- 718 LaRowe, D. E., and P. Van Cappellen (2011), Degradation of natural organic matter: a
719 thermodynamic analysis, *Geochimica et Cosmochimica Acta*, 75(8), 2030-2042.
- 720 Larson, J. H., P. C. Frost, M. A. Xenopoulos, C. J. Williams, A. M. Morales-Williams, J. M.
721 Vallazza, J. C. Nelson, and W. B. Richardson (2014), Relationships between land cover and
722 dissolved organic matter change along the river to lake transition, *Ecosystems*, 17(8), 1413-1425.
- 723 Lehmann, J., and M. Kleber (2015), The contentious nature of soil organic matter, *Nature*,
724 528(7580), 60-68.
- 725 Lin, X., J. McKinley, C. T. Resch, R. Kaluzny, C. L. Lauber, J. Fredrickson, R. Knight, and A.
726 Konopka (2012), Spatial and temporal dynamics of the microbial community in the Hanford
727 unconfined aquifer, *The ISME Journal*, 6(9), 1665-1676.
- 728 Lotspeich, F. B., and B. H. Reid (1980), Tri-tube freeze-core procedure for sampling stream
729 gravels, *The Progressive Fish-Culturist*, 42(2), 96-99.
- 730 Mason, H., J. Begg, R. S. Maxwell, A. B. Kersting, and M. Zavarin (2016), A novel solid-state
731 NMR method for the investigation of trivalent lanthanide sorption on amorphous silica at low
732 surface loadings, *Environmental Science: Processes & Impacts*.
- 733 Minor, E. C., C. J. Steinbring, K. Longnecker, and E. B. Kujawinski (2012), Characterization of
734 dissolved organic matter in Lake Superior and its watershed using ultrahigh resolution mass
735 spectrometry, *Organic Geochemistry*, 43, 1-11.
- 736 Moser, D. P., J. K. Fredrickson, D. R. Geist, E. V. Arntzen, A. D. Peacock, S.-M. W. Li, T.
737 Spadoni, and J. P. McKinley (2003), Biogeochemical processes and microbial characteristics
738 across groundwater-surface water boundaries of the Hanford Reach of the Columbia River,
739 *Environmental Science & Technology*, 37(22), 5127-5134.
- 740 Peterson, R. E., and M. P. Connelly (2004), Water movement in the zone of interaction between
741 groundwater and the Columbia River, Hanford site, Washington, *Journal of Hydraulic Research*,
742 42(S1), 53-58.
- 743 Raffaele, S., A. Leger, and D. Roby (2009), Very long chain fatty acid and lipid signaling in the
744 response of plants to pathogens, *Plant signaling & behavior*, 4(2), 94-99.
- 745 Regnier, P., P. Friedlingstein, P. Ciais, F. T. Mackenzie, N. Gruber, I. A. Janssens, G. G.
746 Laruelle, R. Lauerwald, S. Luyssaert, and A. J. Andersson (2013), Anthropogenic perturbation of
747 the carbon fluxes from land to ocean, *Nature geoscience*, 6(8), 597-607.
- 748 Rood, K., and M. Church (1994), Modified freeze-core technique for sampling the permanently
749 wetted streambed, *North American Journal of Fisheries Management*, 14(4), 852-861.
- 750 Rossel, P. E., C. Bienhold, A. Boetius, and T. Dittmar (2016), Dissolved organic matter in pore
751 water of Arctic Ocean sediments: Environmental influence on molecular composition, *Organic*
752 *Geochemistry*, 97, 41-52.
- 753 Rothman, D. H., and D. C. Forney (2007), Physical model for the decay and preservation of
754 marine organic carbon, *Science*, 316(5829), 1325-1328.
- 755 Schmidt, M. W., M. S. Torn, S. Abiven, T. Dittmar, G. Guggenberger, I. A. Janssens, M. Kleber,
756 I. Kögel-Knabner, J. Lehmann, and D. A. Manning (2011), Persistence of soil organic matter as
757 an ecosystem property, *Nature*, 478(7367), 49-56.

- 758 Shepherd, T., and D. Wynne Griffiths (2006), The effects of stress on plant cuticular waxes, *New*
759 *Phytologist*, 171(3), 469-499.
- 760 Six, J., P. Callewaert, S. Lenders, S. De Gryze, S. Morris, E. Gregorich, E. Paul, and K. Paustian
761 (2002), Measuring and understanding carbon storage in afforested soils by physical fractionation,
762 *Soil science society of America journal*, 66(6), 1981-1987.
- 763 Slater, L. D., D. Ntarlagiannis, F. D. Day - Lewis, K. Mwakanyamale, R. J. Versteeg, A. Ward,
764 C. Strickland, C. D. Johnson, and J. W. Lane (2010), Use of electrical imaging and distributed
765 temperature sensing methods to characterize surface water-groundwater exchange regulating
766 uranium transport at the Hanford 300 Area, Washington, *Water Resources Research*, 46(10).
- 767 Smith, R. M., and S. S. Kaushal (2015), Carbon cycle of an urban watershed: exports, sources,
768 and metabolism, *Biogeochemistry*, 126(1-2), 173-195.
- 769 Stegen, J. C., J. K. Fredrickson, M. J. Wilkins, A. E. Konopka, W. C. Nelson, E. V. Arntzen, W.
770 B. Chrisler, R. K. Chu, R. E. Danczak, and S. J. Fansler (2016), Groundwater-surface water
771 mixing shifts ecological assembly processes and stimulates organic carbon turnover, *Nature*
772 *Communications*, 7.
- 773 Stegen, J. C., X. Lin, A. E. Konopka, and J. K. Fredrickson (2012), Stochastic and deterministic
774 assembly processes in subsurface microbial communities, *The ISME Journal*, 6(9), 1653-1664.
- 775 Tfaily, M. M., R. K. Chu, N. Tolić, K. M. Roscioli, C. R. Anderton, L. Pas□a-Tolić, E. W.
776 Robinson, and N. J. Hess (2015), Advanced solvent based methods for molecular
777 characterization of soil organic matter by high-resolution mass spectrometry, *Analytical*
778 *chemistry*, 87(10), 5206-5215.
- 779 Tfaily, M. M., D. C. Podgorski, J. E. Corbett, J. P. Chanton, and W. T. Cooper (2011), Influence
780 of acidification on the optical properties and molecular composition of dissolved organic matter,
781 *Analytica chimica acta*, 706(2), 261-267.
- 782 Tfaily, M. M., P. Reardon, R. K. Chu, N. Tolić, L. Pas□a-Tolić, E. W. Robinson, and N. J. Hess
783 (2017), Sequential extraction protocol for organic matter from soils and sediments using high
784 resolution mass spectrometry and proton NMR, *Analytica Chimica Acta*.
- 785 Tholl, D. (2015), Biosynthesis and biological functions of terpenoids in plants, in *Biotechnology*
786 *of Isoprenoids*, edited, pp. 63-106, Springer.
- 787 Todd-Brown, K., J. Randerson, W. Post, F. Hoffman, C. Tarnocai, E. Schuur, and S. Allison
788 (2013), Causes of variation in soil carbon simulations from CMIP5 Earth system models and
789 comparison with observations, *Biogeosciences*, 10(3).
- 790 Trail, F., N. Mahanti, and J. Linz (1995), Molecular biology of aflatoxin biosynthesis,
791 *Microbiology*, 141(4), 755-765.
- 792 Tremblay, L. B., T. Dittmar, A. G. Marshall, W. J. Cooper, and W. T. Cooper (2007), Molecular
793 characterization of dissolved organic matter in a North Brazilian mangrove porewater and
794 mangrove-fringed estuaries by ultrahigh resolution Fourier transform-ion cyclotron resonance
795 mass spectrometry and excitation/emission spectroscopy, *Marine chemistry*, 105(1), 15-29.
- 796 Ward, C. P., and R. M. Cory (2015), Chemical composition of dissolved organic matter draining
797 permafrost soils, *Geochimica et Cosmochimica Acta*, 167, 63-79.
- 798 Wieder, W. R., G. B. Bonan, and S. D. Allison (2013), Global soil carbon projections are
799 improved by modelling microbial processes, *Nature Climate Change*, 3(10), 909-912.
- 800 Wieder, W. R., C. C. Cleveland, W. K. Smith, and K. Todd-Brown (2015), Future productivity
801 and carbon storage limited by terrestrial nutrient availability, *Nature Geoscience*, 8(6), 441-444.
- 802 Willaman, J. J., and B. G. Schubert (1961), *Alkaloid-bearing plants and their contained*
803 *alkaloids*, Agricultural Research Service, US Department of Agriculture.

804 Zachara, J. M., P. E. Long, J. Bargar, J. A. Davis, P. Fox, J. K. Fredrickson, M. D. Freshley, A.
805 E. Konopka, C. Liu, and J. P. McKinley (2013), Persistence of uranium groundwater plumes:
806 Contrasting mechanisms at two DOE sites in the groundwater–river interaction zone, *Journal of*
807 *Contaminant Hydrology*, *147*, 45-72.
808 Zhang, L., S. Wang, Y. Xu, Q. Shi, H. Zhao, B. Jiang, and J. Yang (2016), Molecular
809 characterization of lake sediment WEON by Fourier transform ion cyclotron resonance mass
810 spectrometry and its environmental implications, *Water Research*, *106*, 196-203.
811
812

813 **Figures and Tables.**

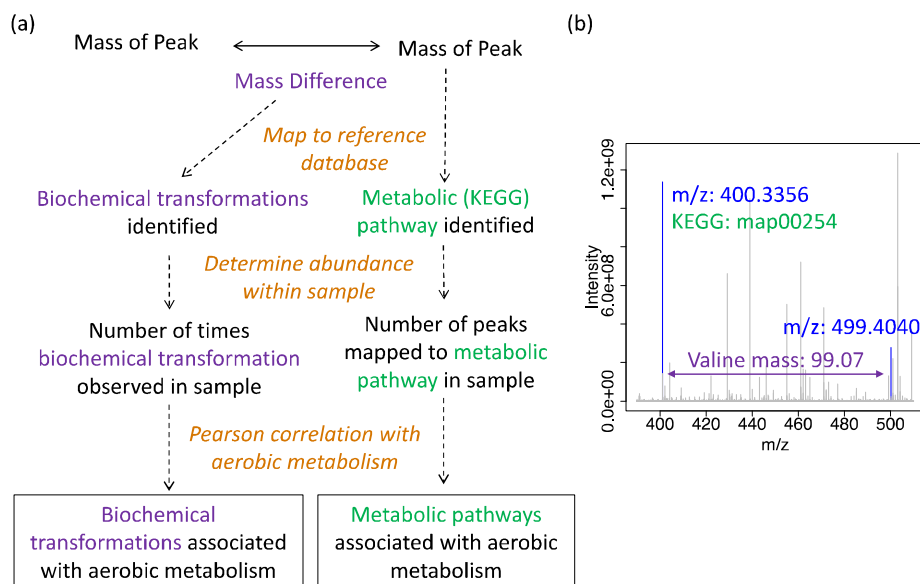
Figure 1



814

815 **Figure 1. NMDS visualization of dissimilarity in OC pool composition.** Water-soluble and
816 bound-OC pools are represented by open circles and x's, respectively. Samples associated with
817 riparian vegetation are blue, and those in areas without vegetation are red. The P-value reflects
818 differences among all groups, as assessed by PERMANOVA. Ellipses represent the standard
819 deviation of the average axis scores for each group, generated using the 'ordiellipse' function in
820 the 'vegan' package. Within each extraction, the composition of OC pools was significantly
821 different across vegetation states (both $P = 0.001$).

822



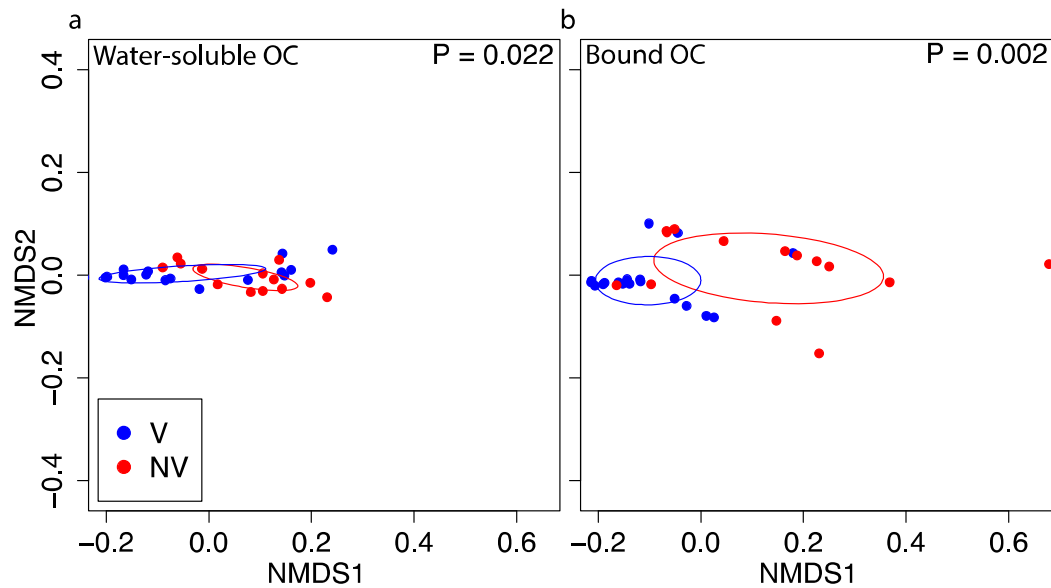
823

824 **Figure 2. Methodology for inferring biochemical transformations and metabolic pathways.**

825 Panel (a) depicts our workflow for analyzing biochemical transformations and metabolic
826 pathways. Biochemical OC transformations (purple) were identified by mapping mass
827 differences in pairwise m/z peak comparisons to a set of 92 known masses transferred in
828 common biochemical transformations (e.g., glucose, amines). Metabolic pathways (green) were
829 identified by mapping all chemical formula assigned to m/z peaks to the KEGG database. Within
830 each sample, the abundance of each biochemical transformation and the number of peaks
831 mapping to each metabolic pathway were then correlated to aerobic metabolism to garner
832 insights into OC oxidation processes. Panel (b) displays an example portion of our FT-ICR-MS
833 spectra overlain with peak assignments (blue), a biochemical transformation (mass difference
834 between peaks, denoted in purple), and a metabolic pathway (associated with the left-hand peak,
835 denoted in green).

836

Figure 3



837

838 **Figure 3. NMDS visualization of biochemical transformation partitioning among vegetation**

839 **states.** Biochemical transformations that were correlated to aerobic metabolism were

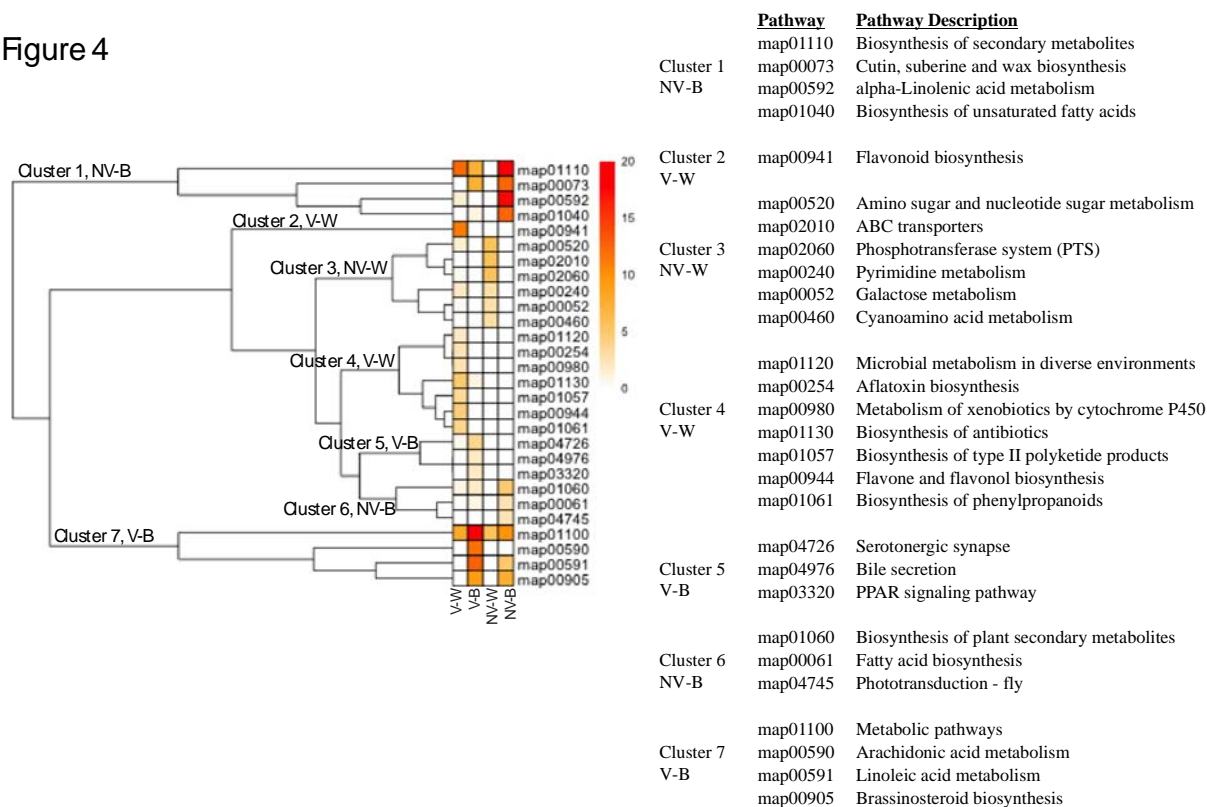
840 significantly different among vegetation states in both the (a) water-soluble and (b) bound-OC

841 pools. V and NV are denoted in blue and red, respectively, and significance values are derived

842 from PERMANOVA. Ellipses represent the standard deviation of the average axis scores for

843 each group, generated using the 'ordiellipse' function in the 'vegan' package.

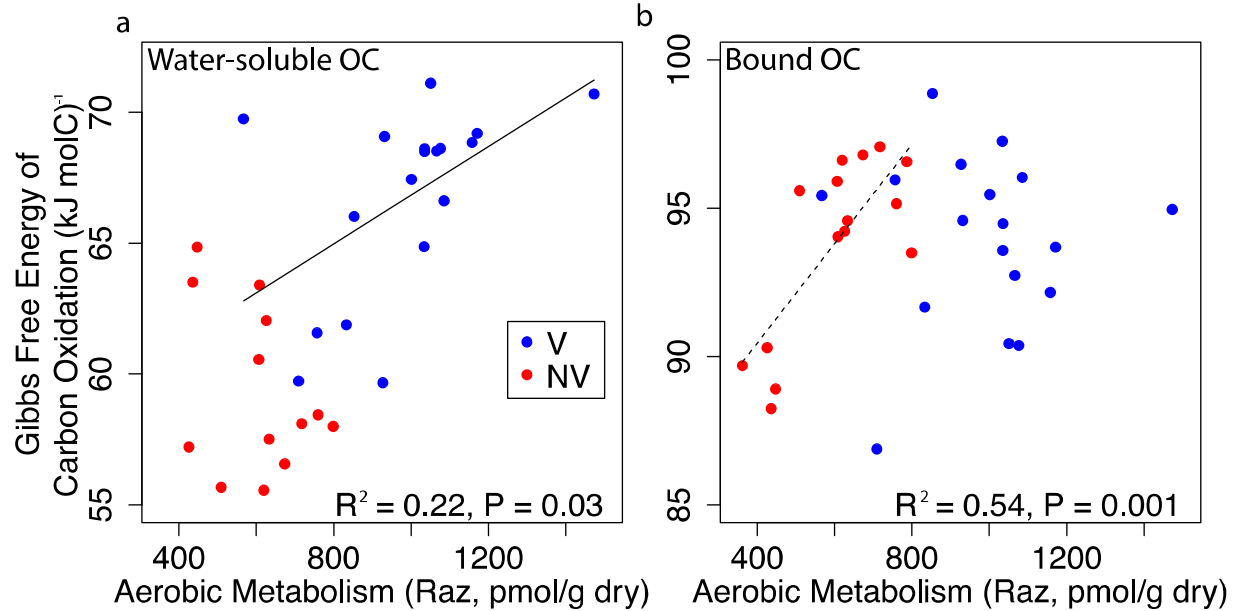
Figure 4



844

845 **Figure 4. KEGG pathways associated with aerobic metabolism.** A hierarchical clustering
 846 heatmap shows KEGG pathways positively associated with aerobic metabolism. Colors move
 847 from white to red from a scale of 0% to 20%, showing percent relative abundance of each
 848 pathway in each group. Pathways are described and divided by cluster and listed in the legend.
 849 V-W, V-B, NV-W, and NV-B are placed on branches that yield clusters with which they are
 850 predominantly associated.

Figure 5



851

852 **Figure 5. Correlations between Gibbs free energy of carbon oxidation ($\Delta G^{\circ}_{\text{Cox}}$) and aerobic**

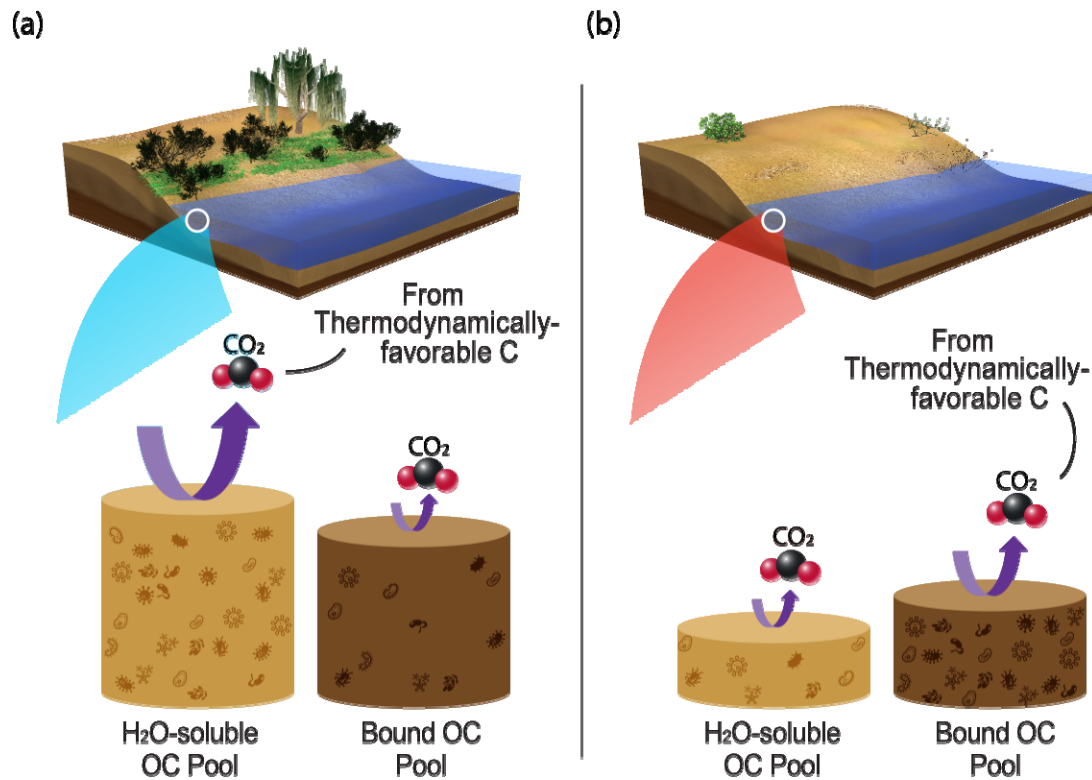
853 **metabolism.** (a) and (b) display linear regressions relating $\Delta G^{\circ}_{\text{Cox}}$ to aerobic metabolism in

854 water-soluble and bound-OC pools, respectively. Aerobic metabolism is expressed as pmoles of

855 resazurin reduced to resorufin per gram dry weight over a 48hr incubation period (Raz, see

856 Supplemental Information). V and NV are denoted in blue and red. Solid lines show significant

857 relationship at V; dashed lines show significant relationship at NV.



858

859 **Figure 6. Conceptualization of relationship between riparian vegetation and OC oxidation.**

860 We propose a conceptualization of OC oxidation at terrestrial-aquatic interfaces whereby (a)
861 more riparian vegetation results in greater terrestrial C deposition and larger water-soluble and
862 bound-OC pools. However, water-soluble OC is preferentially oxidized, which protects the
863 bound-OC pool. Conversely, (b) areas deplete in riparian vegetation experience lower inputs to
864 water-soluble OC pools and show lower rates of OC oxidation. This results in smaller OC pools
865 (water-soluble and bound) and microbial adaptation for oxidation of the bound-OC pool. In both
866 cases, the most thermodynamically favorable portions of the OC pool being metabolized are
867 preferentially oxidized. Height of the cylinders denotes pool sizes, and arrow thickness denotes
868 flux magnitude.

869

870

871 **Table 1. Acronyms and abbreviations used in this paper.**

Abbreviation/Acronym	Description
V	Transect with dense riparian vegetation (i.e., 'vegetated')
NV	Transect with sparse riparian vegetation (i.e., 'not vegetated')
V-W	Transect V, water extraction (water-soluble OC)
V-B	Transect V, chloroform extraction (bound-OC)
NV-W	Transect NV, water extraction (water-soluble OC)
NV-B	Transect NV, chloroform extraction (bound-OC)
H ₂ O	Water
CHCl ₃	Chloroform
C	Carbon
OC	Organic carbon
FT-ICR-MS	Fourier transform ion cyclotron resonance mass spectrometry
KEGG	Kyoto Encyclopedia of Genes and Genomes
$\Delta G^{\circ}_{\text{Cox}}$	Gibbs free energy of C oxidation

873 **Table 2. Biochemical transformations correlated with aerobic metabolism in each OC pool**
 874 **and vegetation state.**

	Pearson's r
V-W	
biotinyl_(-H)_C10H15N2O3S	0.74
uridine_5_diphosphate_(-H2O)_C9H12N2O11P2	0.67
cytosine_(-H)_C4H4N3O	0.65
uridine_5_monophosphate_(-H2O)_C9H11N2O8P	0.65
guanine_(-H)_C5H4N5O	0.61
guanosine_(-H2O)_C10H11N5O4	0.59
adenine_(-H)_C5H4N5	0.59
glutathione_(-H2O)_C10H15N3O5S	0.57
uracil_(-H)_C4H3N2O2	0.56
glucose_C6H12O6	0.53
C6H10O6	0.53
Aspartic_Acid_C4H5NO3	0.52
Glucuronic_Acid_(-H2O)	0.52
Lysine_C6H12N2O	0.51
D-Ribose_(-H2O)_ribosylation)	0.50
secondary_amine	0.50
Alanine_C3H5NO	0.50
C6H10O5	0.49
monosaccharide_(-H2O)	0.49
Threonine_C4H7NO2	0.49
Glutamic_Acid_C5H7NO3	0.48
pentose_C5H8O4	0.47
acetotacetate_(-H2O)_C4H4O2	0.47
Glutamine_C5H8N2O2	0.47
pyridoxal_phosphate_(-H2O)_C8H8NO5P	0.47
V-B	
isoprene_addition_(-H)_C5H7	0.61
phosphate	0.56
primary_amine	0.55
Glucuronic_Acid_(-H2O)	0.53
glyoxylate_(-H2O)_C2O2	0.53
malonyl_group_(-H2O)_C3H2O3	0.52
D-Ribose_(-H2O)_ribosylation)	0.49
pyrophosphate	0.49
acetotacetate_(-H2O)_C4H4O2	0.49
hydrogenation_dehydrogenation_H2	0.47

875

876

NV-W	
NONE	NA
NV-B	
Adenosine_5_monophosphate_(-H2O)_C10H12N5O6P	0.92
adenylate_(-H2O)_C10H12N5O6P	0.92
pyridoxal_phosphate_(-H2O)_C8H8NO5P	0.73
acetylation_(-H2O)_C2H2O	0.70
ketol_group_(-H2O)	0.70
Isoleucine_C6H11NO	0.69
Leucine_C6H11NO	0.69
ethyl_addition_(-H2O)_C2H4	0.69
Threonine_C4H7NO2	0.69
Valine_C5H9NO	0.68
Carboxylation_CO2	0.68
Glycine_C2H3NO	0.67
Formic_Acid_(-H2O)_CO	0.67
Serine_C3H5NO2	0.67
hydroxylation_(-H)_O	0.67
palmitoylation_(-H2O)_C16H30O	0.67
pentose_C5H8O4	0.66
secondary_amine	0.66
condensation/dehydration_H2O	0.66
C2H2_C2H2	0.66
erythrose_(-H2O)	0.66
CH4_O	0.65
methanol_(-H2O)	0.65
glyoxylate_(-H2O)_C2O2	0.65
NH_CH2	0.64
Alanine_C3H5NO	0.63
acetotacetate_(-H2O)_C4H4O2	0.63
Proline_C5H7NO	0.62
hydrogenation_dehydrogenation_H2	0.61
Histidine_C6H7N3O	0.60
malonyl_group_(-H2O)_C3H2O3	0.59
Cysteine_C3H5NOS	0.58
glcnac_C8H13N1O5	0.57
Methionine_C5H9NOS	0.57
Arginine_C6H12N4O	0.56
Aspartic_Acid_C4H5NO3	0.56

D-Ribose(→H₂O)ribosylation)

0.55